Delaminated Zeolites as Support of Active Metals for the Preparation of Highly Active and Selective Catalysts for Hydrogen Production: Steam Reforming of Bioethanol

A. Chica , J.F. Da Costa-Serra, S. Sayas

This document appeared in

Detlef Stolten, Thomas Grube (Eds.):
18th World Hydrogen Energy Conference 2010 - WHEC 2010
Parallel Sessions Book 3: Hydrogen Production Technologies - Part 2
Proceedings of the WHEC, May 16.-21. 2010, Essen
Schriften des Forschungszentrums Jülich / Energy & Environment, Vol. 78-3
Institute of Energy Research - Fuel Cells (IEF-3)
Forschungszentrum Jülich GmbH, Zentralbibliothek, Verlag, 2010
ISBN: 978-3-89336-653-8

Delaminated Zeolites as Support of Active Metals for the Preparation of Highly Active and Selective Catalysts for Hydrogen Production: Steam Reforming of Bioethanol

Antonio Chica*, **Javier Francisco Da Costa-Serra, Salvador Sayas**, Instituto de Tecnología Química (UPV-CSIC), Valencia, Spain

1 Introduction

Hydrogen has attracted much attention as alternative fuel mainly due to environmental aspects. Furthermore, the reserves of fossil fuels on earth are finite and no matter how long they will last, a cleaned and renewable energy alternative independent of fossil fuels has to be developed for the future [1,2]. Currently, the most favourable route to produce hydrogen comes from non-renewable energy sources such as fossil fuels, which is associated with release of large quantities of greenhouse gases to the atmosphere, especially CO_2 and others harmful emissions [3,4]. Thus, a new eco-friendly reservoir of hydrogen is needed for a clean and sustainable production of energy. Biomass-derived compounds such as bioethanol could be this source since it is easy to produce, and is also safe to handle, transport and store [5,6]. Catalytic conversion of bioethanol to hydrogen through steam reforming reaction highly depends on the type of metal catalyst used, type of precursors, preparation methods, type of catalyst support, presence of additives, and operating conditions [6-11]. Among them support plays an important role in the reforming activity since it can help to improve the dispersion of metal catalyst enhancing the metal catalytic activity via metal-support interactions and avoiding the metal sinterization [12]. New delaminated zeolitic materials have been synthesized in our laboratories [13,14]. The singular structure of these delaminated zeolites, and particularly the very high and well-defined external surface area, makes these materials attractive to be used as supports for dispersing active metal phases. In the present work we have explored the activity and selectivity of Co metallic particles supported over two delaminated zeolites (ITQ-2 and ITQ-6) in the steam reforming of bioethanol. The characterization of these materials by DRX, BET area, and TPR has allowed to establish interesting relationships between their catalytic performance and physico-chemical properties.

2 Experimental

2.1 Catalysts preparation and characterization

Pure silica ITQ-2 and ITQ-6 zeolites were prepared as described in [13] and [14], respectively. The incorporation of Co was accomplished by incipient wetness impregnation with an aqueous solution containing the required amount of $Co(NO_3)_2$ $6H_2O$ to achieve a nominal concentration of 20 wt% of Co in the final catalysts. Supports containing Co were

* Corresponding author, email: achica@itq.upv.es

calcined in muffle oven at 873 K for 3 h before reaction. The cobalt content in the calcined samples was determined by atomic absorption spectrophotometry (AAS). Textural properties were obtained from the nitrogen adsorption isotherms determined at 77 K. X-ray diffraction was used to identify the nature of the crystalline cobalt phases.

The reduction properties of the supported oxidized cobalt phases were studied by temperature-programmed reduction (TPR). The degree of reduction was determined from TPR experiments comparing the total amount of hydrogen consumed by each catalyst and the amount of hydrogen theoretically necessary to complete the reduction of Co_3O_4 oxide species present in the catalyst. The metallic particle size was estimated from H_2 adsorption using the double isotherm method. The average Co particle sizes were estimated from the metal's surface area assuming a spherical geometry.

2.2 Catalytic test

Steam reforming experiments were carried out in a continuous fixed bed reactor at atmospheric pressure, H_2O/BioEtOH molar ratio of 13, GHSV 4700 h-1 and a range of temperatures between 673 K and 873 K. Before reaction the catalysts were reduced "in situ" in flow of H_2 at 873 K for 2 hours. The analysis of the compounds of reaction was carried out online using a gas chromatograph equipped with two columns (TRB-5 and CarboSieve SII) and two detectors, thermal conductivity (TCD) and flame ionization (FID). The bioethanol conversion and selectivity to the different reaction products were determined according to the equations (1) and (2), where $(F_{EtOH})_o$ is the flow of bioethanol fed to the reactor, $(F_{EtOH})_f$ the flow of bioethanol that comes from the reactor and F_j the flow of product j that comes from the reactor. Selectivity values were calculated as the molar percentage of the products obtained, excluding water.

$$X(\%, mol) = \frac{(F_{EtOH})_o - (F_{EtOH})_f}{(F_{EtOH})_o} \times 100 \quad (1)$$

$$S(\%, mol) = \frac{F_j}{(\Sigma F_j)_{products}} \times 100 \quad (2)$$

3 Results and Discussion

3.1 Characterization

X-ray diffraction patterns of calcined ITQ-2 (data not shown) does not show the 00l peaks with the 2.5 nm periodicity typical of the MWW topology, indicating a reduction of long-range order along the c axis. These structural changes are in agreement with the proposed structure in which the ITQ-2 material is mostly formed by single layers of the corresponding lamellar precursors. The XRD patterns of calcined ITQ-6 compared to the Ferrierite obtained after calcination of Ferrierite precursor at 853 K (data not shown) show that while the intensities of the reflections corresponding to planes (0kl) were basically unchanged, those corresponding to (h00) have strongly decreased in ITQ-6. This indicates a remarkable loss of

order along the a axis, which would be consistent with a delamination of the layered Ferrierite precursor.

Textural properties of the ITQ-2 and ITQ-6 pattern derived from the N_2 adsorption isotherms are summarized in Table 1. As observed, the original zeolites present a high BET surface area and total pore volume. A reduction of surface area and pore volume is noted in both samples after incorporation of Co. This lost of area can be explained if we assume that Co in calcined zeolites are present in the form of Co_3O_4 and that these phases does not contribute to the surface area [15,16]. Thus, the incorporation of high level of cobalt (20 wt.%) would lead to a dilution effect, which could explain the surface area reduction detected. Pore volume of the samples containing Co is also lower than in the pattern materials. This indicates that a partial plugging of the support pores could also be occurring after Co incorporation.

The X-ray diffractograms (not shown) of the oxidized Co samples (Co/ITQ-2 and Co/ITQ-6) exhibit the reflections characteristic of the spinel Co_3O_4 phase, as it is usually observed for siliceous materials impregnated with cobalt nitrate precursor [17,18]. For comparison purposes, it has been calculated the average diameters of the Co_3O_4 estimated from XRD patterns using the Scherrer equation [19], Table 1. Particle size of Co_3O_4 on Co/ITQ-2 material is found to be smaller than that supported on Co/ITQ-6.

Table 1: Metal content and textural properties of ITQ-2 and ITQ-6 supports and metal-containing catalysts determined by nitrogen adsorption.

Catalyst	Metal content (wt.%)	Surface area (BET) m^2/g	Pore volume (BJH) cm^3/g	Oxide particle size (XRD) (nm)	Metal particle size (H_2-Chemisorption) (nm)
ITQ-2		887	0.72		
ITQ-6		594	0.85		
Co/ITQ-2	20.1	487	0.31	15.9	9.6
CO/ITQ-6	19.5	377	0.42	21.6	14.8

The reduction behaviour of the supported cobalt oxide particles in the catalyst has been studied by temperature-programmed reduction (TPR). The corresponding reduction curves are shown in Figure 1. As observed, both samples present two main reduction features with maxima at about 575 K and 590 K, which correspond to the two-step reduction process in which Co_3O_4 is first reduced to CoO and then CoO is reduced to Co^o, as reported by different authors [18-21]. For Co/ITQ-2 sample the area of the second reduction peak is larger than that for the Co/ITQ-6. Additional broad diffuse hydrogen consumption between 600 K and 1000 K has been also observed both samples, suggesting the existence of several cobalt species reducing at approximately the same temperature, which can be ascribed to the reduction of cobalt silicates probably formed by reaction of highly dispersed CoO with the silica support during the reduction process [18, 22, 23]. The reduction temperature and peak area of this broad peak can be seen that is higher for the Co/ITQ-2 sample. The reduction temperature and the peak width are indications of the degree of reduction and the level of interaction between different species. Thus, TPR results seem to indicate that cobalt oxide

exhibit higher interaction with ITQ-2 support. In the case of Co/ITQ-2 the broad peak detected at higher temperatures suggests that a part of the Co species strongly interact with support resulting difficult their reduction. Taking into a count that the catalysts are reduced at 873 K before reaction it is possible that a part of the Co species in the ITQ-2 support remain in their oxidized form, thus, they could not participate in the bioethanol steam reforming reaction. The low particle-size determined by DRX for the cobalt oxide species supported on ITQ-2 material could also give explanation for the high reduction temperature displayed by part of the supported cobalt. The size of the Co metallic particles was determined by H_2-chemisorption. As it can be seen in Table 1 the smallest Co metallic particles are present in the ITQ-2 support, as it was expected from the lower particle size of the Co oxides detected by DRX for this sample.

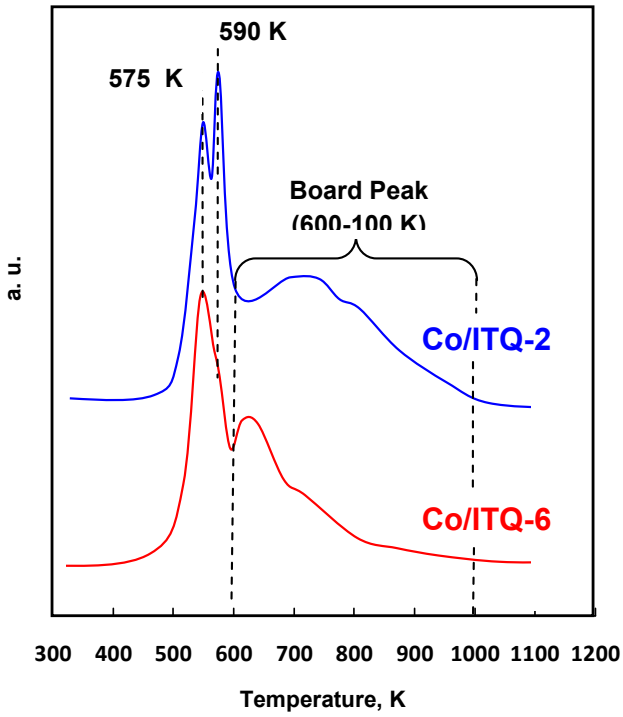

Figure 1: TPR profiles of Co-supported catalysts.

3.2 Catalytic activity

Figure 2 shows the bioethanol conversion as function of the reaction temperature. Co/ITQ-2 sample exhibited higher bioethanol steam reforming activity than Co/ITQ-6 material. Catalytic activity of the cobalt supported catalysts was also compared at 673 K, H_2O/EtOH of 13, GHSV of 4700 h^{-1} and atmospheric pressure. The global reaction rate determined as gram of bioethanol converted per gram of catalyst and per second for the Co/ITQ-2 sample was found to be 2 times higher than that in Co/ITQ-6 (1,8 10^{-2} and 0.9 10^{-2}, respectively). The higher activity of the Co/ITQ-2 sample can be attributed to the small metallic Co particles resulting in a greater density of active metallic surface where the reforming of bioethanol can be carried out. The hydrogen selectivity and catalyst stability are others important

parameters to be taken into account for the practical application of one catalyst. The hydrogen selectivity with reaction temperature is also shown in Figure 2.

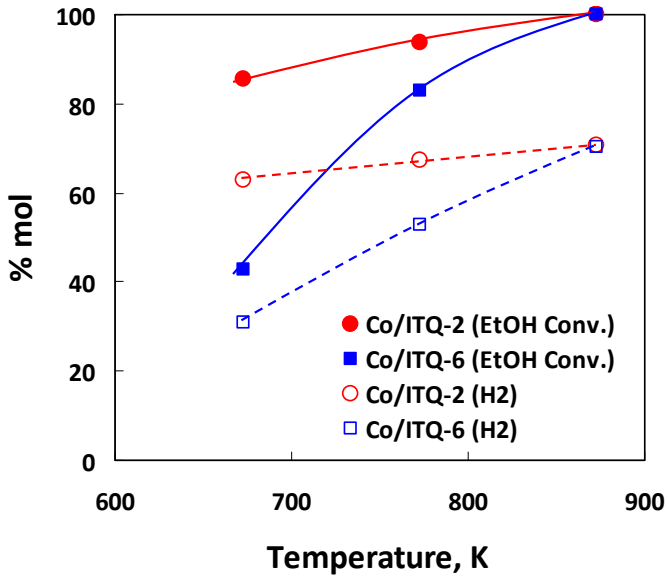

Figure 2: Bioethanol conversion and H_2 selectivity versus reaction temperature. Reaction conditions: H_2O/bioEtOH= 13, GHSV= 4700 h^{-1} and atmospheric pressure.

Both samples showed high hydrogen yields at high temperatures (873 K), however the Co/ITQ-2 was the most selective catalyst to hydrogen at low temperatures. The stability of these catalysts was also tested. It is well known that the stability of a steam reforming catalyst is strongly related to coke deposition and metal sintering. After 72 hour of reaction time at 773 K deactivation was only detected for Co/ITQ-6 catalyst. The elemental analysis of the catalysts after reaction shows the presence of coke in both catalysts. Percentage of carbon was slightly larger for Co/ITQ-6 sample. However, the amount of deposited carbon cannot explain by itself the deactivation exhibited by the Co/ITQ-6 material. Together to the coke deposition it is possible that others effects as metal sinterization could account for the detected deactivation. The best results obtained with the Co/ITQ-2 sample could be due to its particular structure formed by hexagonal array of “cups” (0.7×0.7 nm, see Figure 3), which would provide an excellent position for the stabilization of the Co metallic particles improving their dispersion, decreasing their size and avoiding their sinterization during reduction and reaction steps.

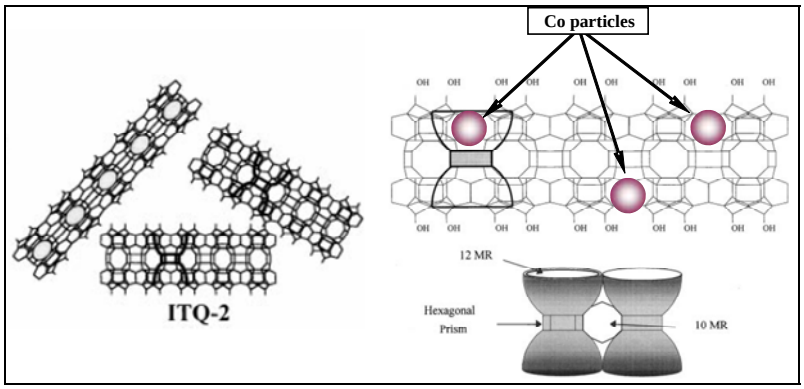

Figure 3: Schematic representation of the Co/ ITQ-2 structure.

The results here presented show that using pure silica delaminated ITQ-2 zeolite as support of Co can be prepared a good bioethanol steam reforming catalyst, with high activity, hydrogen selectivity, and stability, to produce hydrogen.

References

[1] G.W. Huber, A. Corma, *Angew. Chem. Int. Ed.* 46 (2007), pp. 7184.

[2] J. Kjärstad, F. Johnsson, *Energy Policy* 37 (2009), pp. 441–464.

[3] M. H. Kim, E. K. Lee, J. H. Jun, S. J. Kong, G. Y. Han, B. K. Lee, T.-J. Lee, K. J. Yoon, *Int. J. of Hydrogen Energy* 29 (2004), pp. 187–193.

[4] J.R. Rostrup-Nielsen, T. Rostrup-Nielsen, *CATTECH* 6-4 (AUG 2002), pp. 150-159.

[5] A. Midilli, I. Dincer, *Int. J. of Hydrogen Energy* 33 (2008), pp. 4209–4222.

[6] J. Llorca, P.R. de la Piscina, J.A. Dalmon, J. Sales, N. Homs, *Appl. Catal., B* 43 (2003), pp. 355.

[7] A. Birot, F. Epron, C. Descorme, D. Duprez, *Appl. Catal. B* 79 (2008), pp. 17.

[8] G.B. Sun, K. Hidajat, X.S. Wu, S. Kawi, *Appl. Catal. B* 81 (2008), pp. 303.

[9] V. Fierro, V. Klouz, O. Akdim, C. Mirodatos, *Catal. Today* 75 (2002), pp. 141.

[10] A.C. Bagasiannis, P. Panagiotopoulou, X.E. Verykios, *Top. Catal*. 51 (2008), pp. 1.

[11] S. Cavallaro, *Energy Fuels* 14 (2000), pp. 1195.

[12] P.D. Vaidya, A.E. Rodrigues, *Chem. Eng. J.* 117 (2006), pp. 39.

[13] A. Corma, V. Fornés, S.B. Pergher, patent EP 9605004 (1996) and WO 9717290 (1997).

[14] A. Corma, A. Chica, U. Díaz and V. Fornés, patent US6469226 B1 (2002), to BP-AMOCO.

[15] A. Chica, S. Sayas, *Catal. Today* 146 (2009), pp. 37–43.

[16] P. Concepción, C. Lopez, A. Martínez, V.F. Puntes, *J. Catal.* 228 (2004), pp. 321–332.

[17] A.Y. Khodakov, A. Griboval-Constant, R. Bechara, F. Villain, J. Phys. Chem. B 105 (2001) 9805.

[18] B. Ernst, S. Libs, P. Chaumette, A. Kiennermann, Appl. Catal. A 186 (1999) 145.

[19] B.D. Cullity, Elements of X-Ray Diffraction, Addison–Wesley, London, 1878.

[20] R. Riva, H.Miesner, R. Vitali, G. Del Piero, Appl. Catal. A 196 (2000) 111.

[21] D.G. Castner, P.R. Watson, I.Y. Chang, J. Phys. Chem. 94 (1990) 819.

[22] E. van Steen, G.S. Sewell, R.A. Makhothe, C. Micklethwaite, H. Manstein, M. de Lange, C.T. O´Connor, J. Catal. 162 (1996) 220.

[23] B. Sexton, A. Hughes, T. Turney, J. Catal. 97 (1986) 390.